

# Expression Profile of the Embryonic Markers Nanog, OCT-4, SSEA-1, SSEA-4, and Frizzled-9 Receptor in Human Periodontal Ligament Mesenchymal Stem Cells

ORIANA TRUBIANI,<sup>1,2\*</sup> SYLVIA FRANCIS ZALZAL,<sup>3</sup> ROBERTO PAGANELLI,<sup>2</sup> MARCO MARCHISIO,<sup>2,4</sup> RAFFAELLA GIANCOLA,<sup>5</sup> JACOPO PIZZICANNELLA,<sup>2</sup> HANS-JÖRG BÜHRING,<sup>6</sup> MAURIZIO PIATTELLI,<sup>1,2</sup> SERGIO CAPUTI,<sup>1,2</sup> AND ANTONIO NANCI<sup>3</sup>

<sup>1</sup>Department of Oral Science, University of Chieti-Pescara, Chieti, Italy

<sup>2</sup>C.E.S.I., Stem-Tech Group, University "G. d'Annunzio" Foundation, Chieti, Italy

<sup>3</sup>Laboratory for the Study of Calcified Tissues and Biomaterials, Faculty of Dentistry, Université de Montréal, Quebec, Canada

<sup>4</sup>Department of Biomorphology, University "G. d'Annunzio", Chieti, Italy

<sup>5</sup>Department of Transfusion Medicine Civil Hospital, Pescara, Italy

<sup>6</sup>Department of Internal Medicine, Division of Hematology, Oncology, and Immunology, University Clinic of Tübingen, Tübingen, Germany

Mesenchymal stem cells (MSCs) are self-renewing cells with the ability to differentiate into various mesodermal-derived tissues. Recently, we have identified in adult human periodontal ligament (PDL) a population of stem cells (PDL-MSCs) with the ability to differentiate into osteoblasts and adipocytes. The aim of the present work was to further characterize this population and the expression profile of its cells. To achieve our objective we have used flow cytometry, magnetic cell sorting, cytokine antibody array, and light and electron microscope immunostaining. Our results show that the PDL-MSCs contain a subpopulation of frizzled-9 (CD349) positive cells expressing a panel of key mesenchymal and embryonic markers including CD10, CD26, CD29, CD44, CD73, CD90, CD105, CD166, SSEA-1, and SSEA-4. They are additionally positive for nanog and Oct-4; two critical transcription factors directing self-renewal and pluripotency of embryonic stem cells, and they also express the cytokines EGF and IP-10. The presence of nanog, Oct-4, SSEA-1, and SSEA-4 suggests that PDL-MSCs are less differentiated than bone marrow-derived MSCs. Taken together, these data indicate the presence of immature MSCs in PDL and suggest that the frizzled-9/Wnt pathway plays an important role in regulating proliferation and differentiation of these cells.

J. Cell. Physiol. 225: 123–131, 2010. © 2010 Wiley-Liss, Inc.

Mesenchymal stem cells (MSCs) are self-renewing cells which have received much attention because of their multipotency and their potential for diverse clinical applications, including regeneration of bone, cardiac tissue, and treatment of graft versus host disease (Fan et al., 2007). Mesenchymal stem cells have been isolated from various adult and fetal tissues. In culture, they are plastic adherent, assume a spindle shape, and express a panel of key markers including CD105 (endoglin, SH2), CD73 (ecto-5' nucleotidase, SH3, SH4), CD166 (ALCAM), CD29 ( $\beta$  1-integrin), CD44 (H-CAM), CD90 (Thy-1) (Bühring et al., 2007). Depending on the origin and the culture conditions, they also express CD349/frizzled-9, stage-specific embryonic antigen (SSEA)-4, Oct-4, nanog, and nestin (Battula et al., 2007, 2008; Bühring et al., 2007). Oct-4 and nanog, as well as several cell surface markers (SSEA-1, SSEA-4, TRA-1-60, TRA-1-81) have been used to characterize mouse and human embryonic stem cells (ESC) (Carpenter et al., 2003).

Stem cells with MSCs characteristics have been reported in periodontal ligament (PDL) (Ivanovski et al., 2006; Nagatomo et al., 2006). Our previous studies (Trubiani et al., 2005) provided evidence that the PDL contains an accessible niche of MSCs exhibiting features similar to bone marrow-derived MSCs. These cells can differentiate into osteoblasts and

adipocytes, and secrete IL-7 and SDF-1 $\alpha$  (Trubiani et al., 2008a). Teeth develop as epithelial appendages from surface ectoderm, and the molecular mechanisms regulating tooth morphogenesis are shared with other ectodermal organs such as hair, feathers, and scales (Pispa and Thesleff, 2003). Conserved signaling molecules of the Wnt, fibroblast growth factor (FGF), bone morphogenetic protein (BMP), and hedgehog families mediate reciprocal interactions between the epithelial and mesenchymal tissues regulating tooth initiation and morphogenesis (Jernvall and Thesleff, 2000). The Wnt family of growth factors is important in epithelial–mesenchymal interactions which occur during development, and the developing tooth is an excellent model in which to study the

\*Correspondence to: Oriana Trubiani, Department of Oral Science, University of Chieti-Pescara, Via vestini, 31, 66100 Chieti, Italy. E-mail: trubiani@unich.it

Received 16 July 2009; Accepted 5 April 2010

Published online in Wiley InterScience  
(www.interscience.wiley.com.), 21 May 2010.  
DOI: 10.1002/jcp.22203

molecular mechanisms controlling these interactions (Sarkar and Sharpe, 2000). Inhibition of canonical Wnt signaling, either by deleting *Lef1* function or overexpressing the Wnt inhibitor *Dkk1*, arrests tooth morphogenesis at an early stage (Van Genderen et al., 1994; Andl et al., 2002). The activation of Wnt signaling in oral epithelium induces formation of tooth-like buds in chick embryos (Harris et al., 2006), and of Wnt/beta-catenin signaling continuous tooth generation in mouse (Jarvinen et al., 2006).

Frizzled (FZD) proteins comprise a family of transmembrane-spanning receptors (FZD1-10) activated by Wnt ligands (Logan and Nusse, 2004). FZD9 can be activated by Wnt 2 and Wnt 8 via the canonical pathway (Momi et al., 2003), and by Wnt 7 via non-canonical signaling (Winn et al., 2005). Mouse FZD9 is present in the developing brain, in neural precursor cells in the developing neural tube, and in myotomes (Van Raay et al., 2001). In the adult mouse, FZD9 mRNA expression is abundant in the heart, brain, skeletal muscle, kidney, and testis (Wang et al., 1999). In normal tissue, FZD9 protein is found on the surface of pericytes surrounding large blood vessels of human placenta and in bone marrow MSCs (Battula et al., 2007, 2008).

Investigation of the expression patterns of key pluripotency molecules provides insight into the complex network of interacting molecules that regulate cell fate. In this work, we have analyzed the expression of human ESC markers by PDL-MSCs including the transcription factors *nanog* and *Oct-4* as well as the surface molecules SSEA-1 and SSEA-4. Since the Wnt pathway is involved in tooth development, we have also investigated the expression of the CD349/FZD9 receptor.

## Materials and Methods

### Isolation and culture of PDL-MSCs

Human PDL biopsies were carried out after informed consent on five volunteers aged 20–35 years. All subjects were exempt of systemic and oral diseases. Explants were obtained from alveolar crest and horizontal fibers of the PDL by scraping the roots of non-carious third molars with a Gracey's curette (Carranza and Ubios, 2003). The PDL-MSCs were obtained and cultured in MSCM medium (Cambrex Company, Walkersville, MD) according to the manufacturer's instructions (Trubiani et al., 2005, 2008a). Cells migrated from the explants and on day 7 they were 80–90% confluent as determined by phase contrast microscopy. Adherent cells were isolated using 0.1% trypsin solution and plated in tissue culture polystyrene flasks at  $5 \times 10^3$  cells/cm<sup>2</sup>. Primary cultures of PDL mainly consisted of colonies of bipolar fibroblast-like cells which, after subcultivation, proliferated with a population-doubling time of 48 h reaching a confluent growth-arrested condition (Trubiani et al., 2005). Cells developing as an adherent layer were then mechanically detached, and cell viability was evaluated using the trypan blue dye exclusion test.

### Flow cytometry analysis

PDL-MSCs were characterized by multiparameter flow cytometry using FITC-conjugated monoclonal antibodies against CD44, CD90 and PE-conjugated monoclonal antibodies against CD10, CD26, CD29, CD73, CD105, CD166 (Becton-Dickinson, San Jose, CA). In addition, the cells were labeled with the frizzled-9-specific antibody W3C4 and stained with a PE-conjugated secondary step reagent (Becton-Dickinson). Surface expression of SSEA-1 and SSEA-4 and intracytoplasmic expression of *nanog* and *Oct-4* was analyzed using the human ESC marker antibody panel purchased from R&D Systems (Minneapolis, MN). The secondary antibodies were goat anti-mouse IgM (FITC and PE-conjugated), goat anti-mouse IgG FITC and FITC-conjugated donkey anti-goat antibody, all from R&D Systems. One million cells were incubated with antibodies for 30 min at 4°C. Excess antibody was removed by

washing and the stained cells were analyzed on a FACSCalibur flow cytometer (Becton-Dickinson) using CellQuest software. Cut-off markers were set individually for each measurement according to the negative control. Fluorescence intensity for a surface antigen was calculated as the geometric mean (MFI) of all cells above cut off.

### Magnetic activated cell sorting (MACS)

In order to obtain information on cell populations differentially expressing the surface marker FZD9/CD349, PDL-MSCs were separated into positive and negative subsets using the Mini MACS system (Miltenyi Biotec, Bergisch Gladbach, Germany), according to the instructions of the manufacturer. Briefly, cells were resuspended in 0.5% BSA/PBS and incubated with anti-CD349 antibody (10 µg/ml) for 20 min at 4°C, followed by a magnetically labeled goat anti-mouse IgM (Miltenyi Biotec) for 20 min at 4°C. The cells were then washed three times with 0.5% BSA/PBS. For sorting and selection of FZD9/CD349<sup>+</sup> cells, labeled cells were loaded onto a sterile LS column installed in a magnetic field. The column was rinsed with 0.5% BSA/PBS and the negative unlabeled cells passed through. Trapped cells were eluted after the removal of the column from the magnetic field and were collected by centrifugation. For sorting and selection of FZD9/CD349<sup>-</sup> cells, an LD column was used and the negative unlabeled cells were collected in a centrifugation tube. Sorted CD349<sup>+</sup> and CD349<sup>-</sup> cells were grown separately at a density of  $2 \times 10^4$  cells/cm<sup>2</sup> in culture medium. Cells were detached using 0.4% trypsin and stained with 0.05% trypan blue to detect live and dead cells after 24, 48, 72, and 96 h, by using a hemocytometer count of at least three wells in four independent experiments. The supernatants were analyzed for cytokine detection.

### Cytokine detection in culture

The TranSignal Human Cytokine Array 3.0 (Panomics, Inc., Fremont, CA) was used to detect the presence of 36 different cytokines in serum-free supernatants of 24-h recultured second-passage PDL-MSCs, and cells cultured after immunomagnetic separation of CD349<sup>+</sup> from CD349<sup>-</sup> cells. The test was performed according to the manufacturer's instructions: briefly, 2 ml of fivefold dilutions of supernatants were incubated on membranes spotted with antibodies to the cytokines for 2 h, then washed and blocked. Biotin-labeled anti-cytokine mix was then added, followed by Streptavidin-HRP for another 2 h. The reaction was developed with the substrate and the result of exposing the membranes for 12 min was captured using a chemiluminescent imaging system (FluorChem, Alpha Innotech Corp, San Leandro, CA). Negative and positive controls as well as detection reagents were provided with the kit. The 36 molecules present and detectable by the array are indicated in Figure 3 (grid).

### Preparation for scanning electron microscopy

Following cell sorting, the surface characteristics of both CD349<sup>+</sup> and CD349<sup>-</sup> glass-adherent cells was examined. Cells were fixed with 2.5% glutaraldehyde in 0.1 M cacodylate buffer pH 7.4 for 30 min at 4°C, postfixed with 1% osmium tetroxide, dehydrated in a graded series of ethanol, and immersed in isoamyl acetate. They were critical point dried with CO<sub>2</sub>, coated to 3-nm thickness with an osmium plasma coater (Nippon Laser and Electronics Laboratories, Nagoya, Japan), and observed with a Zeiss EVO50 scanning electron microscope.

### Immunofluorescence staining and confocal laser scanning microscope analysis

Cells grown on glass coverslips were fixed for 10 min at RT with 4% paraformaldehyde in 0.1 M sodium phosphate buffer (PBS), pH 7.2. After washing in PBS, cultures were processed for immunofluorescence labeling. Briefly, PDL-MSCs were permeabilized with 0.5% Triton X-100 in PBS for 10 min, followed by blocking with 5% skimmed milk in PBS for 30 min. Primary

monoclonal antibodies to goat anti-nanog and anti-Oct3/4, mouse anti-SSEA-1 and anti-SSEA-4 and anti-human CD349 were used, followed by Alexa Fluor 488 green fluorescence conjugated donkey anti-goat, donkey anti-mouse, and goat anti-mouse as secondary

antibodies (Molecular Probes, Invitrogen, Eugene, OR). Subsequently the PDL-MSCs were incubated with Alexa Fluor 594 phalloidin red fluorescence conjugate (1:400, Molecular Probes), as a marker of the actin cytoskeleton. Before mounting for microscope observation, samples were briefly washed with  $\text{dH}_2\text{O}$  and cell nuclei stained with TOPRO 1:200 (Molecular Probes) for 5 min. The Glass coverslips were placed face down on glass slides and mounted with Prolong antifade (Molecular Probes). Staining was visualized using a Zeiss LSM510 META confocal system (Jena, Germany), connected to an inverted Zeiss Axiovert 200 microscope equipped with a Plan Neofluar oil-immersion objective ( $40\times/1.3$  NA). Images were collected using an argon laser beam with excitation lines at 488 nm and a helium-neon source at 543 and 665 nm.

#### Western blot analysis

Thirty micrograms of proteins from FZD9<sup>+</sup> and FZD9<sup>-</sup> cells were separated on SDS-PAGE and subsequently transferred to nitrocellulose sheets using a semidry blotting apparatus. Sheets were saturated for 60 min at 37°C in blocking buffer (1 × TBS, 5% milk, 0.05% Tween-20), then incubated overnight at 4°C in blocking buffer containing primary antibodies to  $\beta$ -actin, EGF or IP-10 (all from Santa Cruz Biotechnology, Inc., Santa Cruz, CA). After four washes in TBS containing 0.1% Tween-20, samples were incubated for 30 min at room temperature with peroxidase-conjugated secondary antibody diluted 1:2,000 in 1 × TBS, 5% milk, 0.05% Tween-20. Bands were visualized by the ECL method. The level of recovered protein was measured using the Bio-Rad (Hercules, CA) Protein Assay (detergent compatible) according to the manufacturer's instructions.

#### Colloidal gold immunolabeling for SEM analysis

For visualization of the cell surface labeling, cells grown on glass coverslips were fixed and washed in PBS as above, blocked with 5% skimmed milk in PBS for 30 min and incubated with anti-CD349/FZD9 for 2 h at RT. They were then extensively washed in 0.01 M PBS, blocked again with skimmed milk and incubated with protein A-gold complex prepared in-house as described by Bendayan (1995). After washing with 0.1 M PBS, the cells were dehydrated with graded acetone and critical point dried using  $\text{CO}_2$  in a Bal-Tec CPD 030 critical point drier (Bal-Tec AG, Fürstentum, Liechtenstein). The cells were then evaporated with carbon using a Bal-Tec MED 020 coating system (Bal-Tec), and examined using a JEOL JSM 7400F field emission scanning electron microscope operated at 3–5 kV.

#### Statistical analysis

The growth of CD349<sup>+</sup> and CD349<sup>-</sup> cells was analyzed by Sigma Plot 9.0 (Systat Software, Inc., Point Richmond, CA). A *P*-value  $\leq 0.05$  was considered statistically significant.

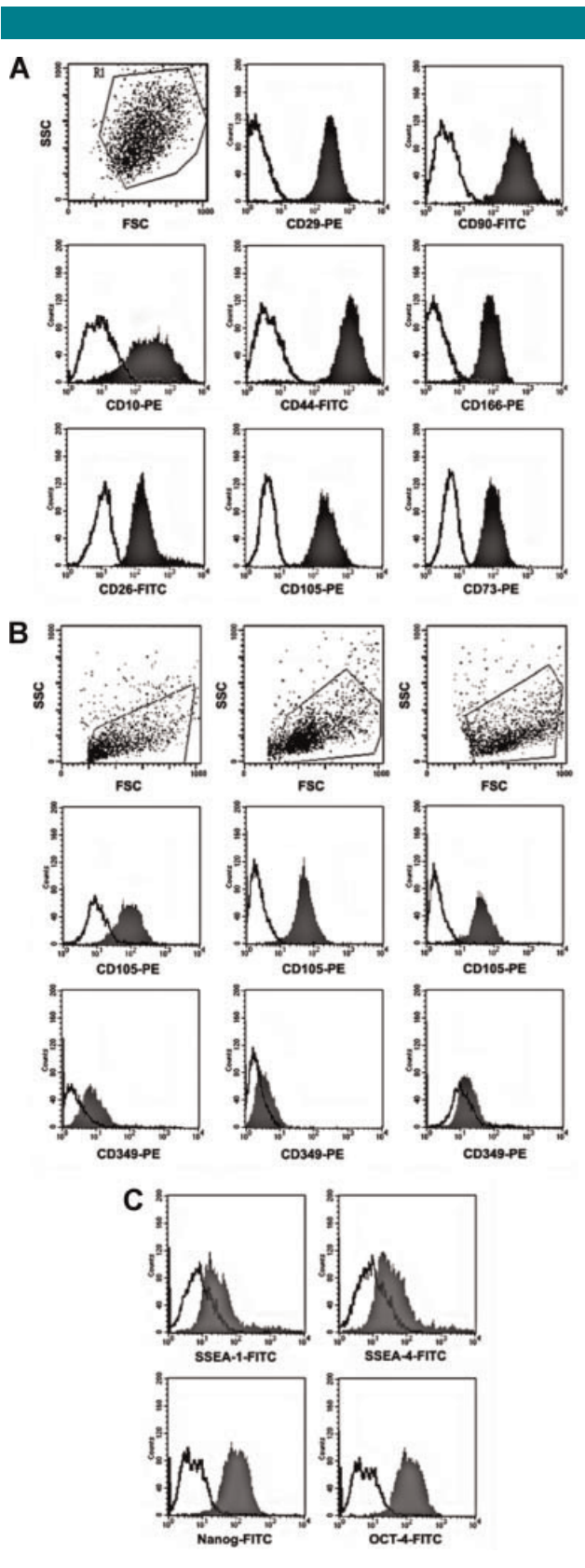


**Fig. 1.** Section A: Cytofluorimetric profile of the surface expression of the mesenchymal-related antigens CD10, CD26, CD29, CD44, CD73, CD90, CD105, and CD166. These data are representative of five separate experiments. Section B: Mesenchymal stem cells isolated from human periodontal ligament were stained with an FZD-9-reactive monoclonal antibody for flow cytometry. Expression of this cell membrane receptor declines after the second cell passage (bottom row, middle part). Comparative analysis of CD105 antigen was also carried out for four separate experiments. Section C: Cytofluorimetric detection of nanog and Oct-4 transcription factors in PDL-MSCs indicating the presence of cells with an immature phenotype. Expression analysis of the cell surface markers SSEA-1 and SSEA-4 confirmed their presence. The data are representative of five separate experiments.

## Results

### Expression analysis by PDL-MSCs

Periodontal ligament mesenchymal stem cells exhibited a cell-surface mesenchymal antigen phenotype positive for CD10, CD26, CD29, CD90, CD44, CD73, CD105, CD166 (Fig. 1A). At the second passage, they expressed the stem cell surface marker CD349/FZD9 and its expression was down-regulated during the subsequent passages (Fig. 1B). Expression of nanog, Oct-4, SSEA-1 and SSEA-4 were also observed (Fig. 1C).

### Immunomagnetic separation

In order to obtain more in depth understanding of the biological significance of the differential expression of CD349/FZD9 by PDL-MSCs, we performed immunomagnetic cell sorting using CD349 antibody (clone W3C4E11). Both purified FZD9<sup>+</sup> and FZD9<sup>-</sup> cell populations were obtained from the primary culture of PDL-MSCs. Cytofluorimetric analysis showed the purity of the FZD9<sup>+</sup> population to be >95% (data not shown). Cells counts and viability are summarized in Figure 2. From 24 h cultures onwards, FZD9<sup>-</sup> cells were shown to be proliferating at higher rates compared with CD349<sup>+</sup> ones, as indicated by the

cell numbers. The decline in CD349 expression with subsequent passages (Fig. 1B) may in part be attributed to higher growth rate of CD349<sup>-</sup> cells.

### Cytokine detection

The following cytokines: IL-12, IL-4, IFN $\gamma$ , TNF $\alpha$ , and MIP4 were detected in control unseparated PDL-MSC cultures (Fig. 3, part A, boxed spots). After sorting into FZD9<sup>+</sup> and FZD9<sup>-</sup> cells and reculturing, these five cytokines were found to still be produced by both subsets. There was, however, a slight decrease in signal intensity for IL-12 and MIP4 in CD349<sup>+</sup> cells (Fig. 3, part B). There were also four cytokines that were not detected in the control (parental) line that were additionally secreted. Two of them, soluble Fas and the matrix metalloproteinase MMP-3, were present in both CD349<sup>+</sup> and CD349<sup>-</sup> subsets, whereas the two others differed, characteristically showing an association with the presence or absence of Wnt receptor CD349/FZD9. CD349<sup>+</sup> cells produced EGF and IP-10 (Fig. 3, boxed spots in part B), whereas CD349<sup>-</sup> MSCs secreted Leptin and sTNFRII (Fig. 3, boxed spots in part C). The results of the apparently CD349/FZD9 specific molecules detected in the array were further examined by Western blot technique, and the expression of EGF and IP-10 in FZD9<sup>+</sup> cells was confirmed (Fig. 3, part D, section A).

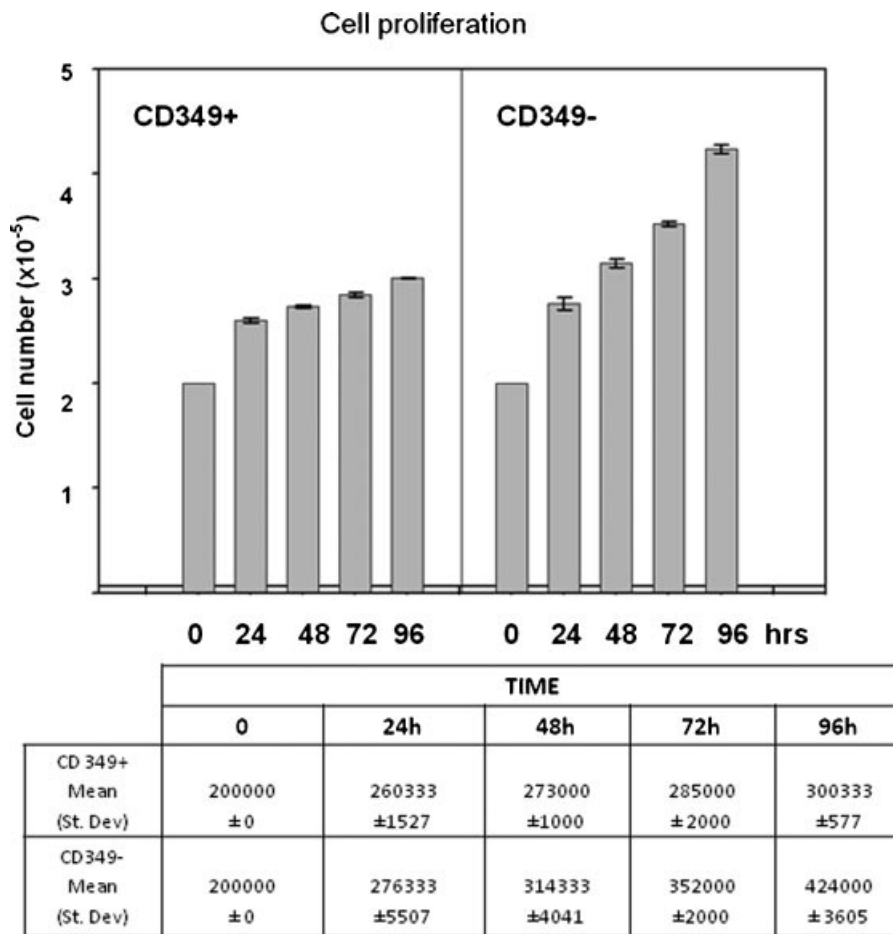


**Fig. 2.** Proliferation rate and viability as determined by the trypan blue exclusion test. Sorted CD349/FZD9<sup>+</sup> cells, at the second passage, showed an overall increase in cell growth starting at 48 h, which differed significantly from the growth profile exhibited by the CD349/FZD9<sup>-</sup> cells. The Y axis shows cell number. Means  $\pm$  standard deviations of four separate experiments were calculate as reported in table. Statistical analysis performed by Anova test indicated significant differences among groups ( $P \leq 0.05$ ).

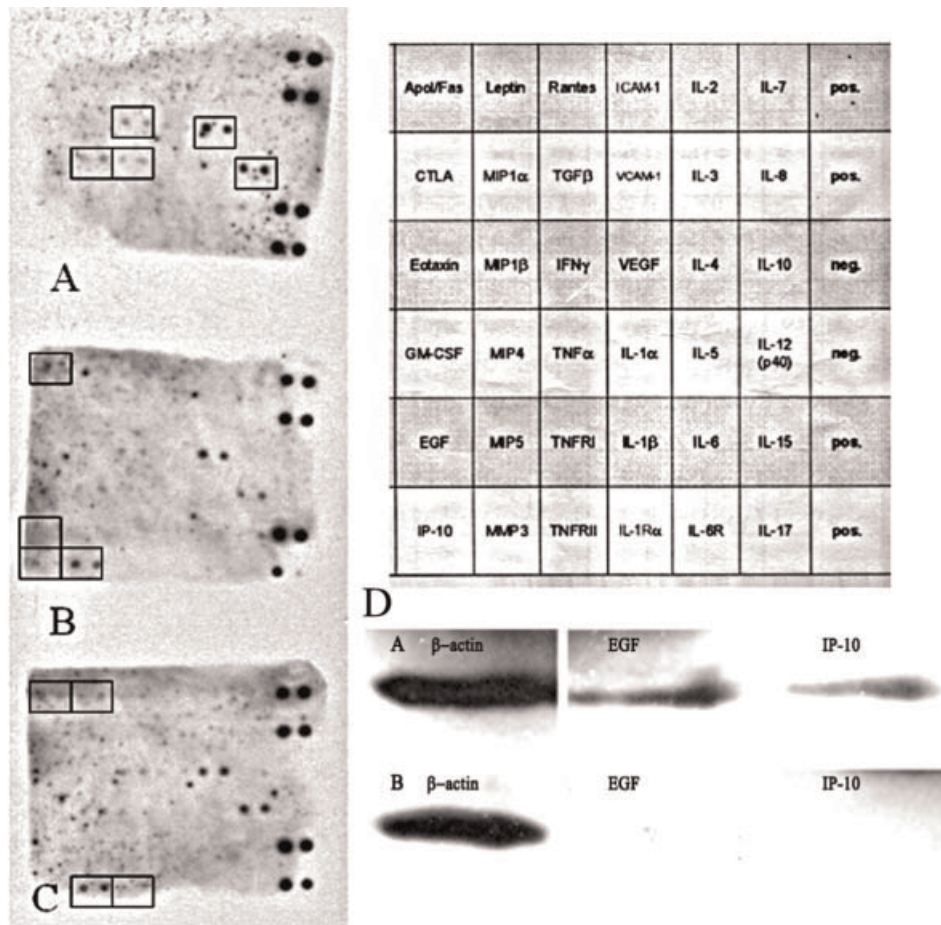


**Fig. 3.** Representative cytokine arrays of second passage PDL-MSCs (A), and separated CD349<sup>+</sup> (B) and CD349<sup>-</sup> cells (C). The 36 different molecules identified in the array and their position are indicated in the grid. The results of a representative proteomic array on total MSCs recultured in serum-free medium for 24 h are reported in part (A), where boxed spots indicate detectable molecules (from top right: IFN $\gamma$ , IL-4, MIP4, TNF $\alpha$ , and IL-12). Part B reports secreted pattern of separated CD349<sup>+</sup> cells, with boxed spots not present in the unseparated MSCs (from top right: Fas, EGF, IP-10, MMP3); finally in part C the boxed spots not present in the parental MSCs (from top right: Fas, Leptin, MMP3, sTNF-R1) in supernatants of separated CD349<sup>-</sup> cells. According to cytokine array, the part D display the western blotting analysis of CD349<sup>+</sup> (A) and CD349<sup>-</sup> cells (B). In part D section A a marked positivity for EGF and IP-10 is present.  $\beta$ -Actin was used as housekeeping protein.

### Cells morphology by scanning electron microscopy

There were morphological differences between the FZD9<sup>+</sup> and FZD9<sup>-</sup> cells. Cultured cells from the FZD9<sup>-</sup> subset were mainly elongated in shape and exhibited one or more major cytoplasmic processes (Fig. 4A). The FZD9<sup>+</sup> cells were more spread and assumed rounded outlines, with sometimes one extremity fanning out (Fig. 4B).

### Immunofluorescence and colloidal gold immunolabeling

Triple-labeled fluorescence preparations of the CD349<sup>+</sup> cells visualized by confocal laser scanning microscopy revealed the FZD9/CD349 labeling as punctuate deposits distributed throughout the cytoplasm and on the cell surface (Fig. 5). The surface localization was confirmed by immunogold labeling FZD9/CD349 and visualization in the scanning electron microscope (Fig. 6). CD349<sup>-</sup> cells showed no reactivity (Fig. 5, inset). In PDL-MSCs, the nanog transcription factor localized strictly as an intense signal in the nucleolus (Fig. 7A) while the Oct-4 transcription factor was found as a punctuated precipitate in the nucleoplasm and cytoplasm (Fig. 7B). Staining for SSEA-1 and SSEA-4 surface antigens was seen in the cytoplasm and on the cell surface (Fig. 7C,D). All labelings

visualized by immunohistochemistry were in agreement with cytofluorimetric results.

### Discussion

The PDL contains postnatal MSCs capable of regenerating several tissues of mesenchymal origin, such as bone, cartilage, and adipose tissue, as well as cementum/PDL-like structures which may take part in periodontal repair (Shi et al., 2005; Inanc et al., 2006). The PDL contributes to tooth nutrition and homeostasis, helps to dampen mastication mechanical forces and plays an important role in adjacent bone remodeling. Periodontal ligament retains a regenerative capacity during adulthood as it contains progenitor cells that maintain their proliferation and differentiation potential into various cell lineages including osteoblasts, fibroblasts, and cementoblasts (Seo et al., 2004; Inanc et al., 2006).

Our group has characterized, phenotypically and functionally, human MSCs isolated from PDL and demonstrated similarities to bone marrow MSCs (Trubiani et al., 2005, 2008a,b; Ivanovski et al., 2006; Nagatomo et al., 2006). In the present study, the characterization of these PDL-MSCs has been extended by analyzing their expression profile for various

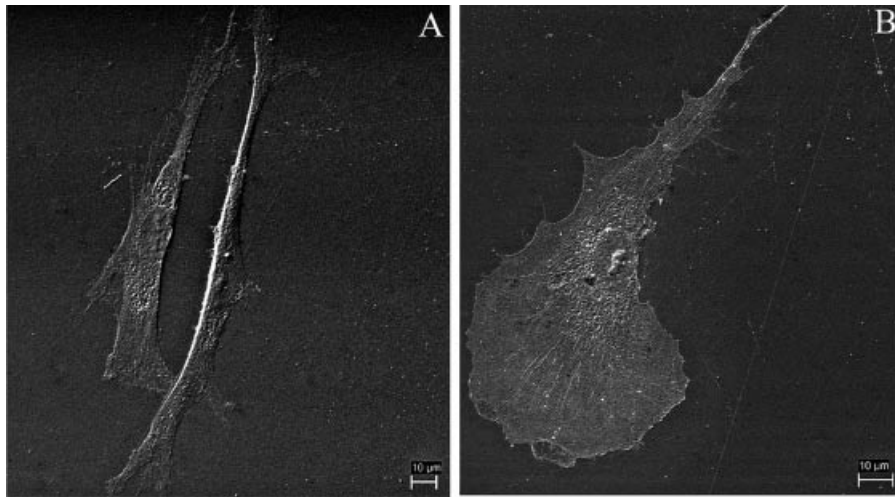


**Fig. 4.** Scanning electron microscope imaging of sorted and (A)  $FZD9^-$  and (B)  $FZD9^+$  human PDL-MSCs. These two subpopulations of PDL-MSCs exhibit different cell morphology.

stem cell markers. Our results show that PDL-MSCs also express several putative markers of bone marrow MSCs, including CD10, CD 26, CD29, CD44, CD73, CD90, CD105, and CD166. A subset of cells also shows the  $FZD9/CD349$  receptor on its surface, and while at the second passage CD349 was clearly expressed, it was down-regulated in subsequent passages. We speculate that the presence of CD349 is related to cell proliferation; in fact, comparative growth analysis of  $FZD9^+$  and  $FZD9^-$  cells suggests a difference in proliferation between these two subpopulations.  $FZD9^-$  cells' higher proliferation rate could induce its prevalence with respect to the  $FZD9^+$  population. It is noteworthy that the pattern of

cytokine secretion we found has not been previously observed in MSCs, although MIP4 (PARC), but not IL-4,  $IFN\gamma$  or  $TNF\alpha$  was described in human cord blood-derived MSCs (Choi et al., 2008) and IL-4 was found to be upregulated in splenocytes by murine MSCs (Liu and Hwang, 2005). IL-7, which we reported at high levels in both bone marrow MSCs and in PDL-MSCs (Trubiani et al., 2008a), was below measurement level under the serumless culture conditions imposed by the filter assay. More interestingly, we consistently detected IL-12 and  $IFN\gamma$ . IL-12 stimulates  $IFN\gamma$  production, and this in turn promotes IP-10 synthesis, which was present in  $FZD9^+$  cells only. The presence of receptors and intracellular signaling molecules for the IL-12/ $IFN\gamma$  pathway in hMSC has not been studied, although Hemedi et al. (2010) reported that upon stimulation with  $IFN\gamma$  immortalized MSC upregulated expression of chemokine receptors and migration. A number of other cytokines was found and they may account for the immunosuppressive functions of MSCs (Apolloni et al., 2000). However, other regulatory cytokines such as IL-10 could not be detected under our experimental conditions (Choi et al., 2008). We also did not observe other expected molecules, such as IL-6, VEGF (Liu and Hwang, 2005) and sVCAM (Juneja et al., 1993).

The differential secretion of molecules such as EGF and IP-10 in  $FZD9^+$  cells may be relevant for their lineage differentiation capacity, and their interaction with other cell types in their natural environmental niche. The pattern of cytokine secretion of  $CD349^-$  cells, including Leptin and sTNFR2, seems to indicate some differentiation towards a preadipocyte phenotype. A similar observation was made using umbilical cord blood MSCs induced by IL-1 beta (Liu and Hwang, 2005) and, as for  $CD349^+$  cells, IP-10 production was observed in un-induced cord blood MSCs (Liu and Hwang, 2005).

An interesting observation concerns detection of the transcription factors nanog and Oct-4. Nanog is a divergent homeodomain protein found in mammalian pluripotent cells and developing germ cells that can orchestrate ESC machinery and it is also considered a core element of the pluripotent transcriptional network (Chambers et al., 2007). This protein, which is found in the nucleoplasm and nucleoli, localizes strictly in trophectoderm nucleoli. This pattern may reflect the down-regulation of protein by sequestration/degradation utilizing a nucleolar mechanism known to operate in stem cells (He et al., 2006). Oct-4 is a master transcriptional regulator,

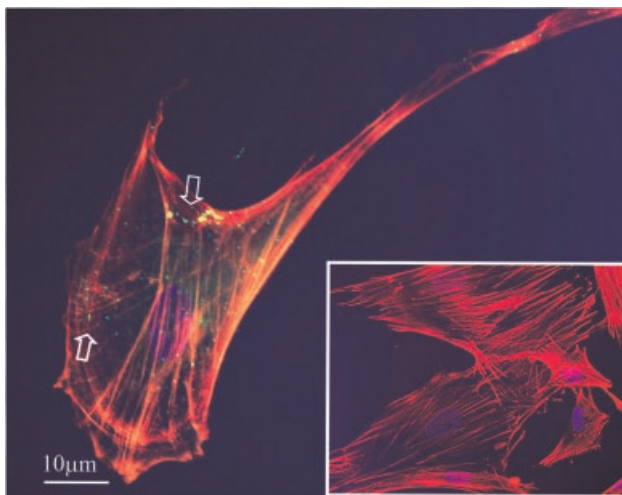


**Fig. 5.** Triple labeling with  $CD349$ /phalloidin/TOPRO (green, red and blue fluorescence, respectively) of PDL-MSCs at the second passage. A punctuate  $CD349$  labeling was clearly observed on the cell membrane. Moreover, there is also a diffuse cytoplasmic staining. The inset shows a negative control following double labeling with phalloidin/TOPRO. Original magnification 40 $\times$ .

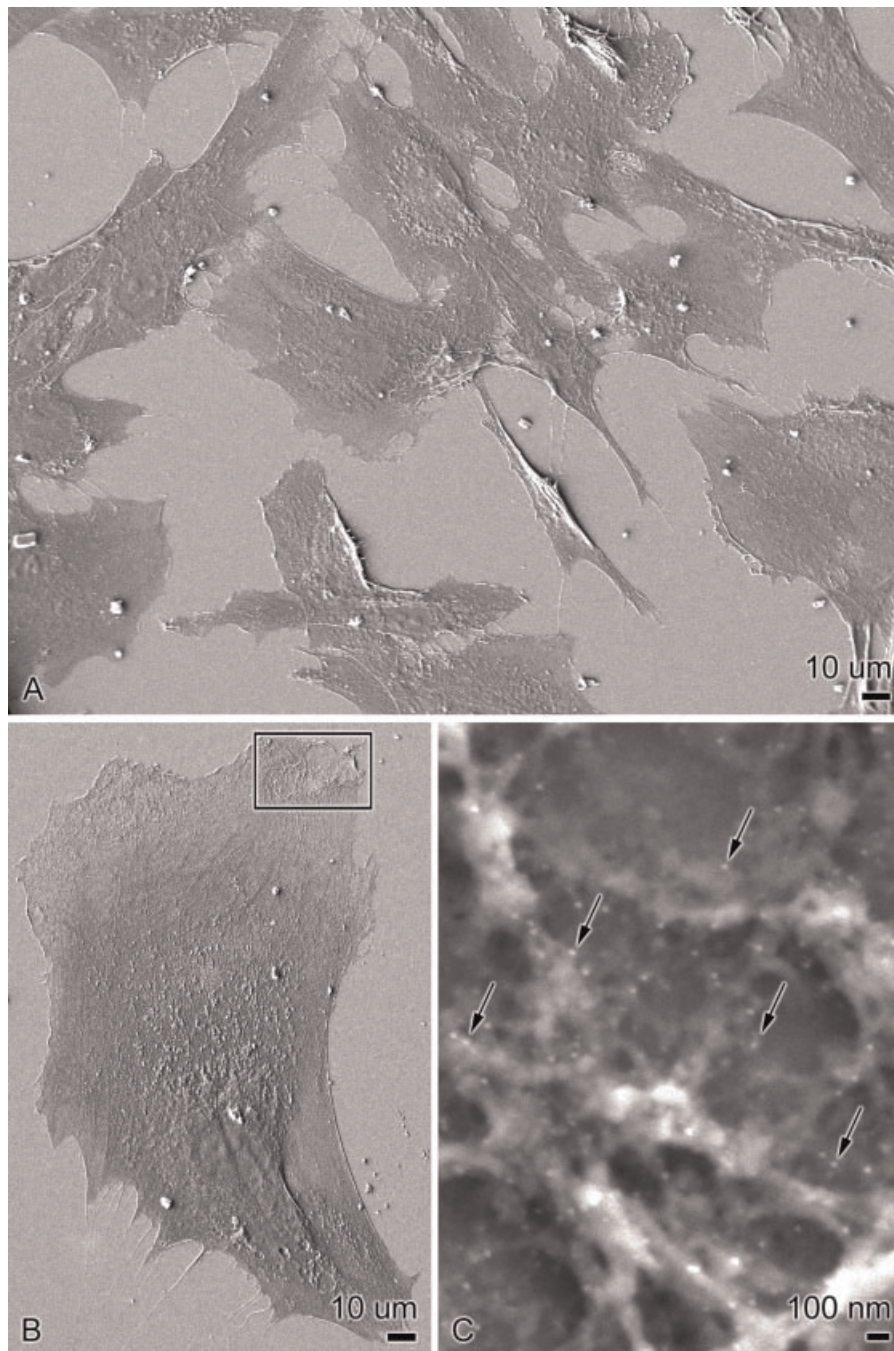


**Fig. 6.** Immunogold labeling for the CD349/FZD9 receptor in PDL-MSCs cultures visualized in the scanning electron microscope. **A:** The cells exhibit a variety of morphologies. **B:** Higher magnification of a typical cell. **C:** Enlargement of the boxed area in (B); gold particles (arrows) are found on the cell surface in certain peripheral regions.

which mediates pluripotency in ESCs through inhibition of tissue-specific and promotion of stem cell-specific genes (Greco et al., 2007). Its expression correlates with cell fate specification and lineage-specific differentiation (Greco et al., 2007). Therefore, the presence of pluripotency markers nanog at the nucleolar level and of Oct-4 at cytoplasmic and nuclear levels in PDL-MSCs suggests that these cells could be less differentiated than classical bone marrow-derived MSCs. We also demonstrated the expression of SSEA-1 and SSEA-4 by PDL-MSCs, two molecules characteristic of undifferentiated

pluripotent human stem cells (Battula et al., 2007, 2008; Gang et al., 2007). SSEA-1 ( $Le^x$ ) is a homophilic adhesion molecule capable of interacting with itself and that is localized preferentially on cell surface projections. Carbohydrate-carbohydrate interactions are important in the specific recognition among cells (Eggens et al., 1989; Kojima et al., 1994) especially during embryogenesis and organogenesis (Knowles et al., 1980). In addition, it has been demonstrated that SSEA-1 may be used as a marker of cell status to test the phenotypic stability of long-term ESC cultures (Cui et al., 2004) and it is

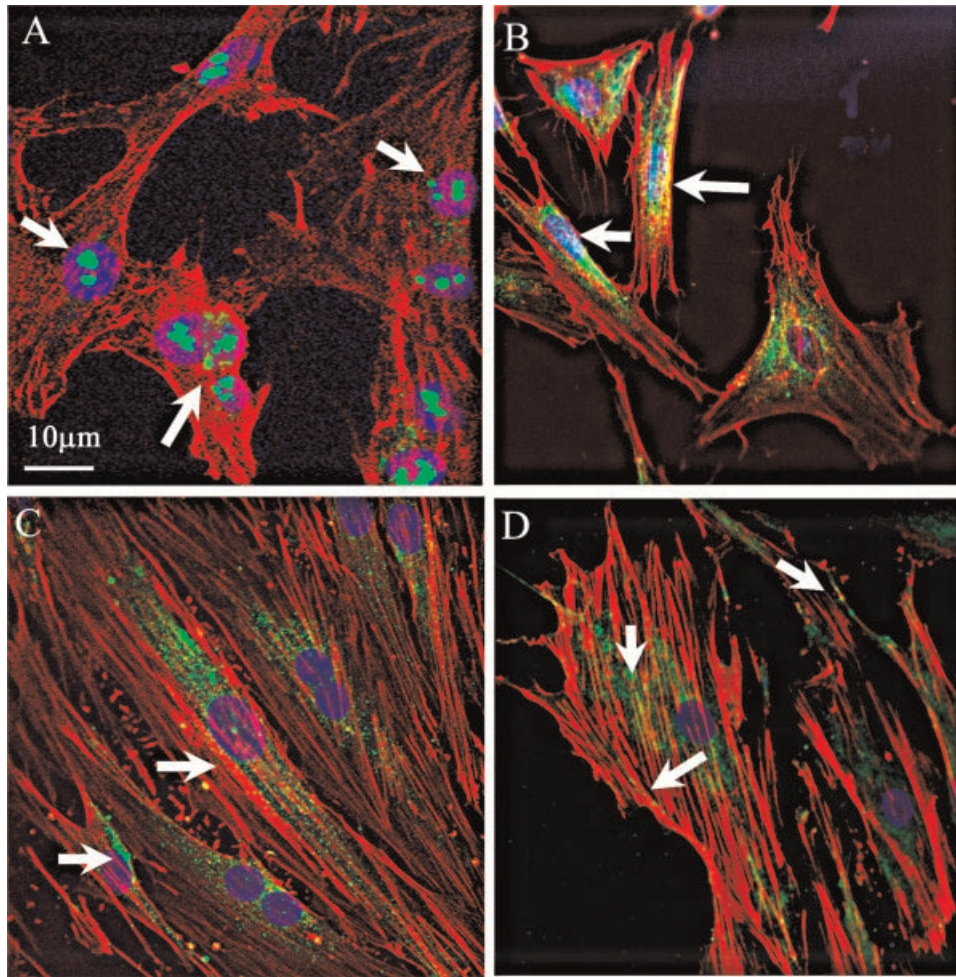


**Fig. 7.** Confocal microscope images of PDL-MSCs. The monolayer was stained with anti-nanog, Oct-4, SSEA-1, and SSEA-4 antibody. **A:** The nanog transcription factor localizes strictly as intense signal in the nucleolus. **B:** Immunoreactivity for the Oct-4 transcription factor is found throughout the nucleoplasm and cytoplasm. **C,D:** Illustrate the distribution SSEA-1 and SSEA-4 surface antigens. In both cases, there specific staining in the cytoplasm and at the cell surface. Nuclei were counterstained with TOPRO and the cytoskeleton with phalloidin. Original magnification: 40 $\times$ .

present in multipotent uterine fibroblasts derived from human placenta (Strakova et al., 2008). Postnatal stem cells identified in various tissues reside in specialized microenvironments or niches endowed with the capacity to maintain stem cell proliferation, and to provide signals for their migration and differentiation. These unique attributes involve a complex array of both paracrine and autocrine signaling molecules, specific cell–cell and cell–extracellular matrix interactions, and biochemical and mechanical stimuli (Kortessidis et al., 2005).

In a recent study on the core transcriptome of MSCs of different origins (including cord and BM) both TGF $\beta$  signaling molecules and the Wnt signaling pathways were prominently expressed (Tsai et al., 2007). It has also been shown that canonical Wnt signaling virtually regulates all of the defined human adult stem cell systems, including skin, blood, intestine, and brain (Radtke and Clevers, 2005; Reva and Clevers, 2005). Although the expression of several Wnt genes in both early oral epithelium and mesenchyme has been described, little is currently known about the role of this signaling pathway in tooth development (Sarkar and Sharpe, 1999). The balance between Wnt ligands and antagonists in undifferentiated odontogenic mesenchyme appears to be important in

controlling tooth bud formation and size (Sarkar and Sharpe, 2000). During root formation, the canonical Wnt signaling inhibits cementoblast differentiation by regulating expression of selective transcription factors. A better understanding of the role of Wnt in cementogenesis may, therefore, open the door to novel strategies for periodontal regeneration and therapies (Nemoto et al., 2009). Our data show that at early stages MSC express ESC markers, but CD349 is only transiently expressed by a subset of cells. Liu et al. (2009) have recently presented an overview of stem cell-related gene expression in dental pulp and periodontal ligament cells during odontogenic/osteogenic differentiation: the implicated genes may interact through the Notch, Wnt, TGF- $\beta$ /BMP, and cadherin signaling pathways to determine the fate of dental-derived stem cells. Moreover, the combination of recombinant WNT protein or WNT mimetic (circular peptide, small molecule, or RNA aptamer) with Notch mimetic compounds, FGF protein, and BMP protein promises to open new tissue engineering avenues for regenerative medicine (Kato, 2008). Our results suggest that the use of specific FDZ9 ligands/inhibitors, and regulators of the IFN $\gamma$  pathway may likewise contribute to such novel therapeutic approaches.

In conclusion, this study describes for the first time the expression of nanog, Oct-4, SSEA-1, and SSEA-4 in human PDL-MSCs. These represent key markers that mediate pluripotency, cell fate specification, and lineage-specific differentiation typical of ESC. These data are particularly important for understanding the molecular machinery involved in dental development. Moreover, the expression of CD349/FZD9 receptor and the secretion of EGF and IP-10 by PDL-MSCs could be central in modulating the intensity of signaling for morphogenetic responses in specialized niches, and in regulating self-renewal, movement and polarity of stem cells. It is plausible that time-regulated expression of the CD349 molecule constitutes a central node during stem cell renewal and differentiation.

### Acknowledgments

This study was supported by the University of Chieti-Pescara Found, Cari-Chieti Foundation (Italy) and in part by the Canadian Institutes of Health Research.

### Literature Cited

- Andl T, Reddy ST, Gaddapara T, Millar SE. 2002. WNT signals are required for the initiation of hair development. *Dev Cell* 2:643–653.
- Apolloni E, Bronte V, Mazzoni A, Serafini P, Carabrelle A, Segal DM, Young HA, Zanovello P. 2000. Immortalized myeloid suppressor cells trigger apoptosis in antigen-activated T lymphocytes. *J Immunol* 165:6723–6730.
- Battula VL, Bareiss PM, Tremel S, Conrad S, Albert I, Hojak S, Abele H, Schewe B, Just L, Skutella T, Bühring HJ. 2007. Human placenta and bone marrow derived MSC cultured in serum-free, b-FGF-containing medium express cell surface frizzled-9 and SSEA-4 and give rise to multilineage differentiation. *Differentiation* 75:279–291.
- Battula VL, Tremel S, Abele H, Bühring HJ. 2008. Prospective isolation and characterization of mesenchymal stem cells from human placenta using a frizzled-9-specific monoclonal antibody. *Differentiation* 76:326–336.
- Bendayan M. Colloidal gold post-embedding immunocytochemistry. *Prog Histochem Cytochem* 1995. 29:1–159.
- Bühring HJ, Battula VL, Tremel S, Schewe B, Kanz L, Vogel W. 2007. Novel markers for the prospective isolation of human MSC. *Ann NY Acad Sci* 1106:262–271.
- Carpenter MK, Rosler E, Rao MS. 2003. Characterization and differentiation of human embryonic stem cells. *Cloning Stem Cells* 5:79–88.
- Carranza FA, Ubios AM. 1996. The tooth-supporting structures. *Clinical periodontology*. Philadelphia: Saunders Company. pp 30–51.
- Chambers I, Silva J, Colby D, Nichols J, Nijmeijer B, Robertson M, Vrana J, Jones K, Grotewold L, Smith A. 2007. Nanog safeguards pluripotency and mediates germline development. *Nature* 450:1230–1234.
- Choi JJ, Yoo SA, Park SJ, Kang YJ, Kim WU, Oh IH, Cho CS. 2008. Mesenchymal stem cells overexpressing interleukin-10 attenuate collagen-induced arthritis in mice. *Clin Exp Immunol* 153:269–276.
- Cui L, Johkura K, Yue F, Ogiwara N, Okouchi Y, Asanuma K, Sasaki K. 2004. Spatial distribution and initial changes of SSEA-1 and other cell adhesion-related molecules on mouse embryonic stem cells before and during differentiation. *J Histochem Cytochem* 52:1447–1457.
- Eggers I, Fenderson BA, Toyokuni T, Hakomori S. 1989. A role of carbohydrate-carbohydrate interaction in the process of specific cell recognition during embryogenesis and organogenesis: A preliminary note. *Biochem Biophys Res Commun* 158:913–920.
- Fan VH, Tamama K, Au A, Littrel R, Richardson LB, Wright JW, Wells A, Griffith LG. 2007. Tethered epidermal growth factor provides a survival advantage to mesenchymal stem cells. *Stem Cells* 25:1241–1251.
- Gang EJ, Bosnakovski D, Figueiredo CA, Visser JW, Perlingeiro RC. 2007. SSEA-4 identifies mesenchymal stem cells from bone marrow. *Blood* 109:1743–1751.
- Greco SJ, Liu K, Rameshwar P. 2007. Functional similarities among genes regulated by OCT4 in human mesenchymal and embryonic stem cells. *Stem Cells* 25:3143–3154.
- Harris MP, Hasso SM, Ferguson MW, Fallon JF. 2006. The development of archosaurian first-generation in a chicken mutant. *Curr Biol* 16:371–377.
- He S, Pant D, Schiffmacher A, Bischoff S, Melican D, Gavin W, Keefer C. 2006. Developmental expression of pluripotency determining factors in caprine embryos: Novel pattern of NANOG protein localization in the nucleolus. *Mol Reprod Dev* 73:1512–1522.
- Hemeda H, Jacob M, Ludwig A, Giebel B, Lang S, Brandau S. 2010. Interferon-gamma and tumor necrosis factor-alpha differentially affect cytokine expression and migration properties of mesenchymal stem cells. *Stem Cells Dev* 19. DOI:1089.scd.2009.0365.
- Inanc B, Elcin AE, Elcin YM. 2006. Osteogenic induction of human periodontal ligament fibroblasts under two- and three-dimensional culture conditions. *Tissue Eng* 12:257–266.
- Ivanovski S, Gronthos S, Shi S, Bartold PM. 2006. Stem cells in periodontal ligament. *Oral Dis* 12:358–363.
- Jarvinen E, Salazar-Ciudad I, Birchmeier W, Taketo MM, Jernvall J, Thesleff I. 2006. Continuous tooth generation in mouse is induced by activated epithelial Wnt/beta-catenin signaling. *Proc Natl Acad Sci USA* 103:18627–18632.
- Jernvall J, Thesleff I. 2000. Reiterative signaling and patterning during mammalian tooth morphogenesis. *Mech Dev* 92:19–29.
- Juneja HS, Schmalsteig FC, Lee S, Chen J. 1993. Vascular cell adhesion molecule-1 and VLA-4 are obligatory adhesion proteins in the heterotypic adherence between human leukemia/lymphoma cells and marrow stromal cells. *Exp Hematol* 21:444–450.
- Katoh M. 2008. WNT signaling in stem cell biology and regenerative medicine. *Curr Drug Targets* 9:565–570.
- Knowles BB, Pan S, Solter D, Linnenbach A, Croce C, Huebner K. 1980. Expression of H-2, laminin and SV40 T and TASA on differentiation of transformed murine teratocarcinoma cells. *Nature* 288:615–618.
- Kojima T, Michiue T, Orihara M, Saigo K. 1994. Induction of a mirror-image duplication of anterior wing structures by localized hedgehog expression in the anterior compartment of *Drosophila melanogaster* wing imaginal discs. *Gene* 148:211–217.
- Kortesidis A, Zannettino A, Isenmann S, Shi S, Lapidot T, Gronthos S. 2005. Stromal-derived factor-1 promotes the growth, survival, and development of human bone marrow stromal stem cells. *Blood* 105:3793–3801.
- Liu CH, Hwang SM. 2005. Cytokine interactions in mesenchymal stem cells from cord blood. *Cytokine* 32:270–279.
- Liu L, Ling J, Wei X, Wu L, Xiao Y. 2009. Stem cell regulatory gene expression in human adult pulp and periodontal ligament cells undergoing odontogenic/osteogenic differentiation. *J Endod* 35:1368–1376.
- Logan CY, Nusse R. 2004. The Wnt signaling pathway in development and disease. *Ann Rev Cell Dev Biol* 20:781–810.
- Momoi A, Yoda H, Steinbeisser H, Fagotto F, Kondoh H, Kudo A, Driever W, Furutani-Seiki M. 2003. Analysis of Wnt 8 for neural posteriorizing factor by identifying Frizzled 8c and Frizzled 9 as functional receptors for Wnt8. *Mech Dev* 120:477–489.
- Nagatomo K, Komaki M, Sekiya I, Sakaguchi Y, Noguchi K, Oda S, Muneta T, Ishikawa I. 2006. Stem cells properties of human periodontal ligament cells. *J Periodont Res* 41:303–310.
- Nemoto E, Koshikawa Y, Kanaya S, Tsuchiya M, Tamura M, Somerman MJ, Shimauchi H. 2009. Wnt signaling inhibits cementoblast differentiation and promotes proliferation. *Bone* 44:805–812.
- Pispa J, Thesleff I. 2003. Mechanism of ectodermal organogenesis. *Dev Biol* 262:195–205.
- Radtke F, Clevers H. 2005. Self-renewal and cancer of the gut: Two sides of a coin. *Science* 307:1904–1909.
- Reva T, Clevers H. 2005. Wnt signaling in stem cells and cancer. *Nature* 434:843–850.
- Sarkar L, Sharpe PT. 1999. Expression of Wnt signaling pathway genes during tooth development. *Mech Dev* 85:197–200.
- Sarkar L, Sharpe PT. 2000. Inhibition of WNT signaling by exogenous Mfrzb I protein affects molar tooth size. *J Dent Res* 79:920–925.
- Seo BM, Miura M, Gronthos S, Bartold PM, Bataouli S, Brahimi J, Young M, Robey PG, Wang CY, Shi S. 2004. Investigation of multipotent postnatal stem cells from human periodontal ligament. *Lancet* 364:149–155.
- Shi S, Bartold PM, Miura M, Seo BM, Robey PG, Gronthos S. 2005. The efficacy of mesenchymal stem cells to regenerate and repair dental structures. *Orthod Craniofac Res* 8:191–199.
- Strakova Z, Livak M, Krezalek M, Ichnatovych I. 2008. Multipotent properties of myofibroblast cells derived from human placenta. *Cell Tissue Res* 332:479–488.
- Trubiani O, Di Primio R, Traini T, Pizzicannella J, Scarano A, Piattelli A, Caputi S. 2005. Morphological and cytofluorimetric analysis of adult mesenchymal stem cells expanded ex vivo from periodontal ligament. *Int J Immunopathol Pharmacol* 18:213–221.
- Trubiani O, Isgro A, Zini N, Antonucci I, Aiuti F, Di Primio R, Nanci A, Caputi S, Paganelli R. 2008a. Functional interleukin-7/interleukin-7Ralpha, and SDF-1alpha/CXCR4 are expressed by human periodontal ligament derived mesenchymal stem cells. *J Cell Physiol* 214:706–713.
- Trubiani O, Orsini G, Zini N, Di Iorio D, Piccirilli M, Piattelli A, Caputi S. 2008b. Regenerative potential of human periodontal ligament derived stem cells on three-dimensional biomaterials: A morphological report. *J Biomed Mater Res A* 87:986–993.
- Tsai MS, Hwang SM, Chen KD, Lee YS, Hsu LW, Chang YJ, Wang CN, Peng HH, Chang YL, Chao AS, Chang SD, Lee KD, Wang TH, Wang HS, Soong YK. 2007. Functional network analysis of the transcriptome of mesenchymal stem cells derived from amniotic fluid, amniotic membrane, cord blood, and bone marrow. *Stem Cells* 10:2511–2523.
- Van Genderen C, Okamura RM, Fariñas I, Quo RG, Parslow TG, Bruhn L, Grosschedl R. 1994. Development of several organs that require inductive epithelial-mesenchymal interactions is impaired in Lef-1-deficient mice. *Genes Dev* 8:2691–2703.
- Van Raay TJ, Wang YK, Stark MR, Rasmussen JT, Francke U, Vetter ML, Rao MS. 2001. Frizzled 9 is expressed in neural precursor cells in the developing neural tube. *Dev Genes Evol* 211:453–457.
- Wang YK, Spörle R, Paperna T, Schughart K, Francke U. 1999. Characterization and expression pattern of the frizzled gene Fzd9, the mouse homolog of FZD9 which is deleted in Williams-Beuren syndrome. *Genomics* 57:235–248.
- Winn RA, Marek L, Han SY, Rodriguez K, Hammond M, Van Scoyk M, Acosta H, Mirus J, Barry N, Bren-Mattison Y, Van Raay TJ, Nemenoff RA, Heasley LE. 2005. Restoration of WNT-7a expression reverses non-small cell lung cancer cellular transformation through frizzled-9 mediated growth inhibition and promotion of cell differentiation. *J Biol Chem* 280:19625–19634.